INVESTIGATION OF FACTORS INFLUENCING THE FORMATION OF WELD DEFECTS IN NON-VACUUM ELECTRON BEAM WELDING*

U. REISGEN[1], M. SCHLESER[1], A. ABDURAKHMANOV[1], G. TURICHIN[2], E. VALDAITSEVA[2], F.-W. BACH[3], T. HASSEL[3] and A. BENIYASH[3]

[1]Aachen University, Welding and Joining Institute, Aachen, Germany
[2]Saint-Petersburg State Polytechnic University, Institute of Welding and Laser Technology, RF
[3]Leibniz University of Hannover, Institute of Materials Science, Garbsen, Germany

The influence of welding condition parameters and properties of material on formation of defects, such as humping and undercuts, in non-vacuum electron beam welding was investigated. The influence of separate welding parameters on the quality of welds was determined.

Keywords: *non-vacuum electron beam welding, welding speed, power density, shielding gas, weld defects, humping, undercuts*

Nowadays the modern technologies of electron beam welding (EBW) are a very widespread tool for treatment of materials. One of the unique types of EBW is the EBW in the open atmosphere (non-vacuum EBW — NV-EBW), developed more than 50 years ago [1] and basically applied in mass production of light structures [2], in particular in automobile industry in welding of exhaust systems, transmission parts and other components [3, 4]. This process is also applied in production of welded pipes, in welding of hot-rolled strips and structural steels [5]. The basic advantages of NV-EBW as compared to conventional EBW in vacuum are the absence of need in creation of vacuum in working chamber, high speed of welding, small working cycle, good overlapping of gap of welded edges by a beam, high efficiency factor of the equipment. The disadvantages of the process can be small working distance, formation of X-ray radiation and ozone which require facilities with ventilation system protected from radiation.

Due to a large reserve of power the very high speeds of NV-EBW of thin-sheet metals can be theoretically achieved. However, as works [6, 7] show, the intensive dynamics of weld pool at high speed of welding leads to formation of surface weld defects, especially to humping (Figure 1, *a*) and undercuts (Figure 1, *b*). These defects are observed in welding of steel at the speeds of more than 8 m/min, and for aluminium alloys — more than 15 m/min. These phenomena restrict the application of a full potential of power and economic efficiency of NV-EBW technologies.

Experimental installation. For experimental research at the Institute of Materials Science the installation of the type NV-EBW 25-175 TU of the company «PTR-Precision Technology» was used (Figure 2, *b*). The maximum beam power of this system is 25 kW at accelerating voltage U_{acc} = 175 kV and maximum welding speed v_w = 20 m/min. The installation can function both in pulsed and also in continuous conditions. The inclination angle of EB gun can vary from 0 to 90° [5]. At the Welding and Joining Institute of Aachen the «Steigerwald» company equipment was used (Figure 2, *a*). The maximal power of electron beam of this system is 30 kW at accelerating voltage U_{acc} = 150 kW, beam current I_b = 200 mA, maximal reached speed v_w = 57 m/min [4].

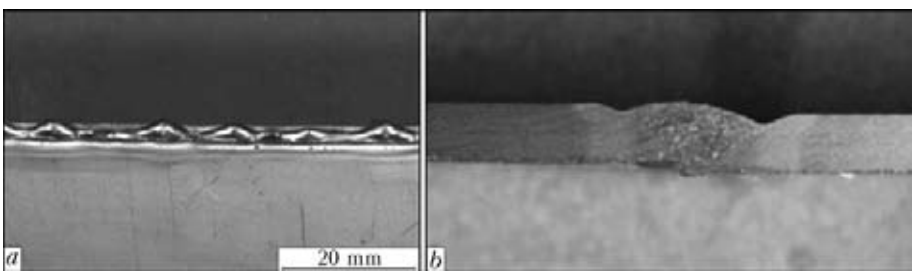

Figure 1. Dynamic defects of welds: *a* — humping (v_w = 10 m/min); *b* — undercut (v_w = 12 m/min)

*Basing on the paper presented at the Int. Conf. on Laser Technologies in Welding and Materials Processing (22–27 May 2011, Katsively, Crimea, Ukraine).

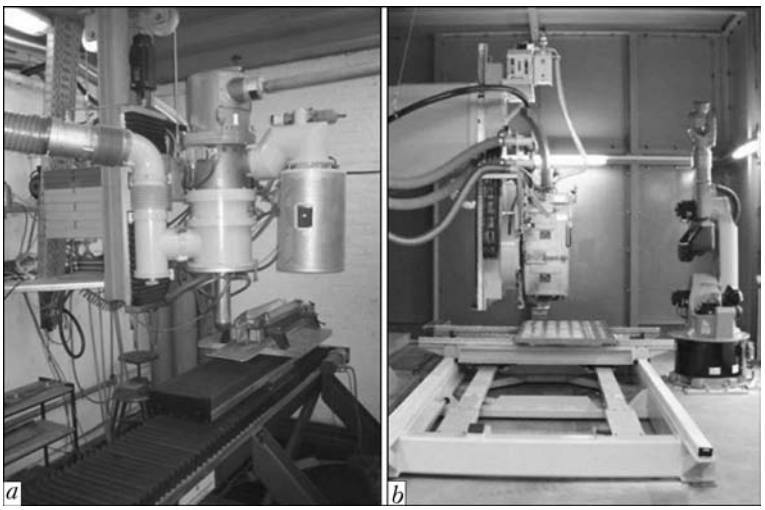

Figure 2. Experimental installations for EBW in open air: *a* — Anlage Type IGM G 150 K («Steigerwald»); *b* — 25-175 TU («PTR-Precision Technology»)

Investigation and modeling of surface dynamics of weld pool. *Shape of free surface of weld pool.* Basing on the equation of Navier–Stokes for the flow of a melt, the equations of continuity of flowing of a melt and conditions of balance of pressures on the free surface, as is shown in [8], the equation was derived describing the shape of a surface of weld pool:

$$\frac{\partial^3 \zeta}{\partial x^3} + \left(\frac{\rho v_0^2}{\sigma H} - \frac{2}{b^2} \right) \frac{\partial \zeta}{\partial x} = -\frac{3}{2LH} + 3\nu \frac{\rho v_0}{\sigma H^2}. \qquad (1)$$

The designations of parameters are presented in Figure 3.

After solution of the equation (1) it is possible to determine the higher level of a melt above the surface of specimen in the tail of weld pool:

$$\zeta \big|_{x=L} = \frac{-\frac{3}{2}\frac{H}{L} + 3\frac{G}{\mathrm{Re}}}{G - 2\frac{H^2}{b^2}} \times$$

$$\times \left(L - 2H \frac{1 - \cos\left(G - 2\frac{H^2}{b^2} \right)^{1/2} \frac{L}{H}}{\left(G - 2\frac{H^2}{b^2} \right)^{1/2} \sin\left(G - 2\frac{H^2}{b^2} \right)^{1/2} \frac{L}{H}} \right), \qquad (2)$$

where $G = (\rho v_0^2)/(\sigma/H)$ is the relation of high-speed pressure of flow of a melt to capillary pressure; v_0 is the speed of a melt relatively to a solid phase, connected with melt flowing round the crater formed under the beam, and can be evaluated in accepted one-dimensional approximation as $v_0 = v_w \frac{h}{H}$, where h is the crater depth.

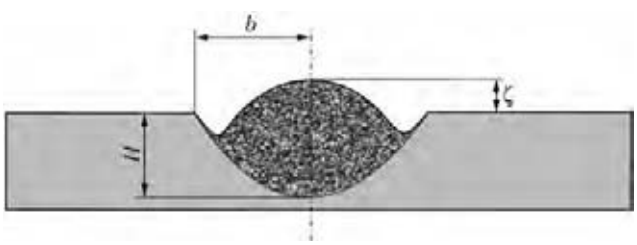

Figure 3. Designation of parameters of weld pool section

The equation (2) allows evaluation of the influence of material properties and geometry of weld pool on reinforcement of a weld.

Let us consider the case of «shallow» and «wide» weld pool, when $G > (2H^2)/b^2$, i.e. when the depth of penetration is less than the width of weld pool. In this case the waves at $(G - (2H^2)/b^2)L/H > 2\pi$ can be formed on the melt surface. Moreover, the middle line of the surface is lowered in direction to the pool tail. In case of a «deep» weld pool, when $G < (2H^2/b^2)$ (depth reaches one third of the width and more), the situation changes radically. The lowering of middle line is changed to its lifting to the end of the pool, the maximal height of which can reach $\frac{3}{2}\frac{b^2}{H}$. One should pay attention to the case when $G \approx (2H^2/b^2)$. Then the height level can be even sufficiently higher. These conditions are the most dangerous from the point of view of unstable formation of surface, but it is impossible to analyze this using accepted approximations of «boundary layer».

This model describes the shape of weld pool at relatively low speeds of welding (welding speed before formation of humping and low weld reinforcements ζ). For experimental verification the welding experiment with relative parameters was carried out. On the produced weld a long-wave profile of the welding bead is observed (Figure 4).

In principle, the given analysis is a theoretical description of process of formation of «stationary» lowering and lifting of weld surface, i.e. formation of undercuts. To analyze the quite non-stationary phenomena, such as humping, it is necessary to preserve

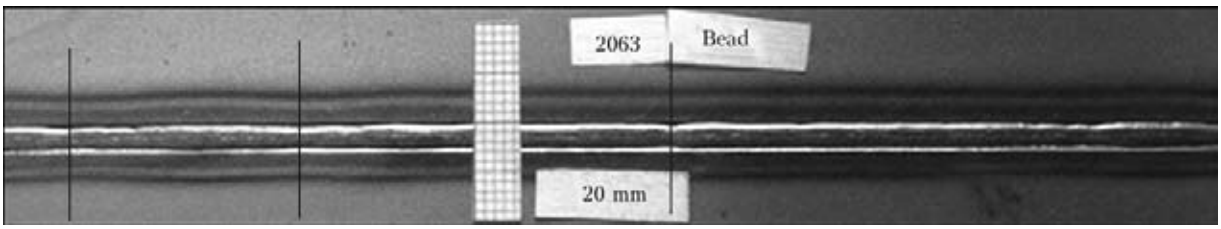

Figure 4. Surface of weld at welding speed before formation of humps (DC05 1.5 mm thick, v_w = 10 m/min, I_b = 70 mA, A = 15 mm)

«non-stationary» members with temporary derivatives and to analyze the stability of «quasi-stationary» behavior, described above.

Stability of weld pool surface. To analyze the stability of weld pool surface, the equation for local lifting of its surface above the surface of specimen was used, derived on the basis of the non-stationary equation of Navier–Stokes, equation of discontinuity and balance of pressures

$$\frac{\partial^2\zeta}{\partial t^2} = -\frac{\sigma H\partial^4\zeta}{\rho\partial x^4} + \frac{2\sigma H\partial^2\zeta}{\rho b^2\partial x^2} + \frac{3\sigma\partial\zeta}{2\rho LH\partial x}. \qquad (3)$$

The designations used in the equation (3) are shown in Figure 5. The analysis of stability of solution of this equation by Lyapunov (stability of flat surface of weld pool) showed that on the surface of weld pool the waves are developed, described by the expression

$$\zeta = \zeta_0 e^{i(\omega t - kx)},$$

where $\omega = \pm\Omega \pm i\gamma$ is the angular frequency. The frequency of waves is preset by expression

$$\Omega = \sqrt{\frac{\sigma H}{\rho}}\left[\left(k^4 + \frac{2k^2}{b^2}\right)^2 + \frac{9k^2}{4L^2H^4}\right]^{1/4} \times \cos\left(\frac{1}{2}\operatorname{arctg}\frac{3b^2}{2LH^2k(k^2b^2+2)}\right). \qquad (4)$$

The increment of waves γ is determined by expression

$$\gamma = \sqrt{\frac{\sigma H}{\rho}}\left[\left(k^4 + \frac{2k^2}{b^2}\right)^2 + \frac{9k^4}{4L^2H^4}\right]^{1/4} \times \sin\left(\frac{1}{2}\operatorname{arctg}\frac{3b^2}{2LH^2k(k^2b^2+2)}\right). \qquad (5)$$

The expressions (4) and (5) determine the conditions and speed of humps growth. As far as the solution of equation (3) contains always the members of the type $e^{\gamma t}$ and $e^{-\gamma t}$, then at any character of γ there is a solution, increasing with time. This means that the presence of Marangoni flow at the surface leads to originating of oscillating instability on it which becomes a reason of humping. The parameters of humping, such as distance between humps and their size, are determined by wave number k (length of exciting waves), which in its turn determines the maximal value of increment γ (maximal speed of growth of disturbances). Thus, humps grow with such wave number which corresponds to maximal speed of growth (humps at a low speed grow also, but they are not seen as far as big humps absorb the small ones). In view of finiteness of length of weld pool L should be selected from the values $k = 2\pi n/L$, where n = 1, 2, 3, ..., m. It is obvious that maximal k value exist on the real axis, which does determine the parameters of humping.

The analysis of expression for increment of wave growth shows that k value providing maximum of increment γ, at made assumptions, depends only on length, width and depth of the weld pool.

As an example let us analyze the process of development of humping with increase of welding speed. The possible lengths of waves on the surface of weld pool are shown in Figure 6 in a form of vertical lines (markers). The speeds of growth of these waves are determined by corresponding values of waves increment. With increase of welding speed, leading to elongation of weld pool, all markers are shifted in the plot to the left, here the speeds of waves growth of different length change and after transition by marker of the longest wave through the maximum its speed begins

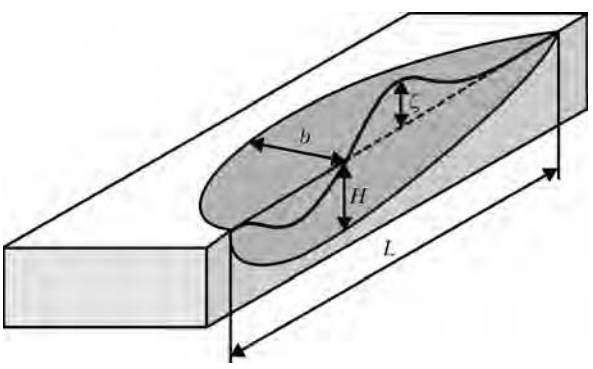

Figure 5. Designations of parameters to the model of weld humping

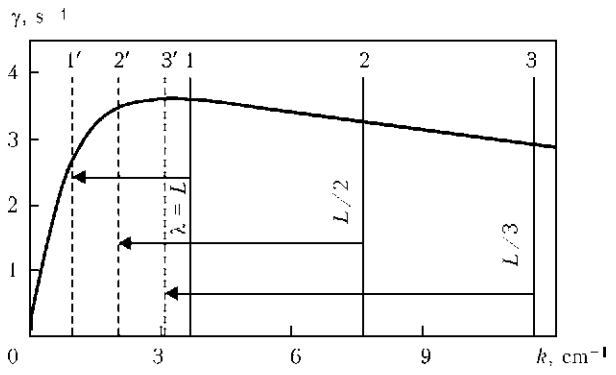

Figure 6. Dependence of increment of wave growth on wave number (for description see the text)

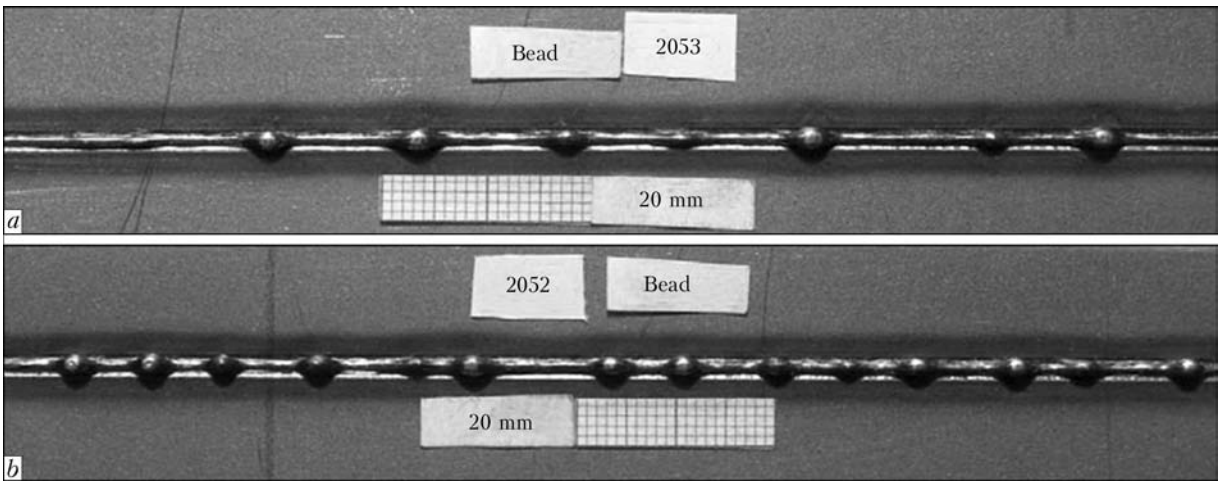

Figure 7. Dependence of humps formation on welding speed (respectively, on weld pool length) at A = 10 mm: a — v_w = 12 m/min, I_b = 65 mA; b — v_w = 15 m/min, I_b = 5 mA

to decrease, which with further increase of welding speed leads to replacement of long-wave humping to short-wave one, i.e. to multifold decrease of distance between the humps. The solid vertical lines in Figure 6 show wave number for short weld pools and dash lines — for long pools. In the long weld pool the short waves are growing quicker, while the long ones are growing in the short pool.

The constructed model can be illustrated by a real example. The growth increment is changed with increase in length of weld pool according to Figure 6. During experiments with a short weld pool (Figure 7, *a*) a wave with $\lambda = L$ is located on the right to the maximum on the plot, therefore it grows faster. At a long weld pool the waves with $\lambda = L$ (Figure 7, *b*) are shifted to the left part from maximum function $\gamma(k)$, i.e. increment of hump growth at wave length L is lower than for waves of length $L/2$.

Experimental investigations. In accordance with the theory given above the basic parameters influencing formation of defects, such as humping and undercut, are length, depth and width of the weld pool. Their values determine threshold speed of welding, at which defects connected with dynamics of pool are still not observed.

Determination of critical speed of welding at different parameters. The results of experiments, carried out on low-carbon steel DC05, showed that with increase of welding speed first the undercuts appear, and achieving the certain critical speed for given parameters of welding the first large humps are formed with non-regular distances between them. With increase of welding speed the number of humps per weld length grows, i.e. frequency of their appearance is increased, the distance between them decreases and sizes of the humps themselves decrease (Figure 8).

The next important parameter is a working distance A, which influences the power density in heating spot. With increase of working distance the density of power sharply increases [9]. The results of experiment show that with decrease of working distance it is necessary to decrease the beam current to maintain the required depth of metal penetration. Here, a weld is already produced and threshold of humping changes not considerably.

The determination of boundary of formation of humps for different materials was carried out similarly to the methods applied for the steel DC05. The experiments showed that there is a certain dependence of critical speed of welding on material being welded (Table 1).

Whereas the threshold of speed of formation of humps for steels is within the limits of 10–12 m/min and depends inconsiderably on chemical composition, even at 20 m/min no humps were observed in welding of aluminium alloy and lead. It is obvious that the

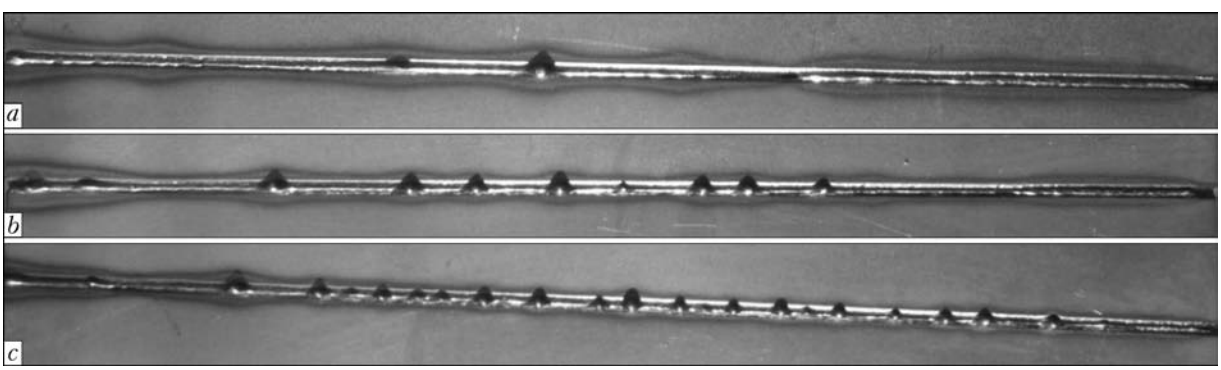

Figure 8. Formation of humps and undercuts at different speed of welding of steel DC05 at U_{acc} = 150 kV, I_b = 100 mA, A = 10 mm: a — v_w = 14; b — 16; c — 18 m/min

Table 1. Influence of material type on critical speed of humps formation

Material	d, mm	v_w, m/min	ρ, J/cm^3	I_b, mA	σ*, mN/m	Notes
Steel DC05	1.5	12	7.874	80	1800	Beginning of humping
Steel TRIP 700	1.5	12	7.874	75	1800	Same
Cu	1.5	15	8.920	68	1250	»
$AlMg_3$	1.7	20	2.660	40	865	Humping was not obtained
Pb	1.0	20	11.340	12.5	451	Same

*Surface tension of pure materials (Fe, Cu, Al, Pb).

Table 2. Influence of material thickness on threshold of speed of formation of weld humping (A = 15 mm, consumption of helium — 90 min^{-1})

Material	d, mm	I_b, mA	v_w, m/min	Notes
DC05	0.7	57	20	Normal weld
DC05	1.5	80	12	Undercut, humping
DC05	3.5	75	6	Same
$AlMg_3$	1.5	40	20	Small undercuts
$AlMg_3$	4.0	70	10	Undercut, humping
Pb	1.0	12.5	20	Small undercuts
Pb	5.5	40	15	Undercut, humping

threshold of speed of humps formation depends on physical properties of material itself and, first of all, on surface tension. It is seen from Table 1 that with decrease of surface tension the threshold of humping is shifted to the region of high speeds of welding which confirms the abovementioned conclusion about leading role of thermal capillary effect at formation of humping in a shallow weld pool. It is indirectly confirmed by dependence of threshold of humping on thickness of material. The results of experiments on determination of influence of thickness of metal on dynamics of weld pool are presented in Table 2.

It was established that threshold of speed of formation of humps drops with increase in thickness of material. It can be explained by change of mechanism of heat conductivity in metallic sheet during transition from two to three dimensional case. The dynamics of weld pool is changed on which, despite surface thermal capillary effect, the convection flows from the bottom of pool to surface influence.

The surface-active substances, such as oxygen in welding of steels, are acting as element decreasing forces of surface tension, moreover, according to Rayleigh theory [10] the critical length of a pool increases ($\lambda > 2\pi R$) and formation of humps can be avoided or their formation shifted to high speeds of welding. At decrease of surface tension the radius is increased and also the critical length, i.e. pool will freeze earlier than a wave will occur. Figure 9 shows the example of influence of Ar + 4 % O_2 gas on formation of humping in the overlap joint.

The investigations showed that application of shielding gas allows increasing the welding speed by 2 m/min earlier than humping is formed.

The conclusion about the fact that Marangoni effect is a decisive factor for dynamics of weld pool is proved also by the following experiment. It is known that sulphur and carbon considerably influence the surface tension of weld pool [11]. Coming from it, a graphite sprayer was used for experiments to cover the half of a metal plate. After welding pass it was revealed that on the part of the plate not covered with graphite the humps were formed, whereas on the part of a plate, treated with graphite, the humps were not observed (Figure 10). As far as the time typical of NV-EBW is very short, one can neglect the influence of diffusive processes and come simply from surface effects.

High-speed video record of weld pool. Using the high-speed video record of weld pool carried out in

Figure 9. Influence of shielding gas on hamps formation in overlap joint (steel S420MC 2 mm thick, v_w = 10 m/min, shots behind the welding process): *a*, *b* — without shielding gas; *c*, *d* — with Ar + O_2 gas

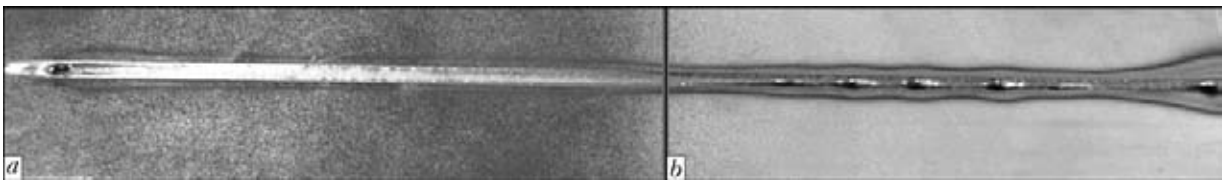

Figure 10. Influence of surface-active substance on dynamics of weld pool (DC05 1.5 mm thick, v_w = 14 m/min) with (*a*) and without (*b*) graphite

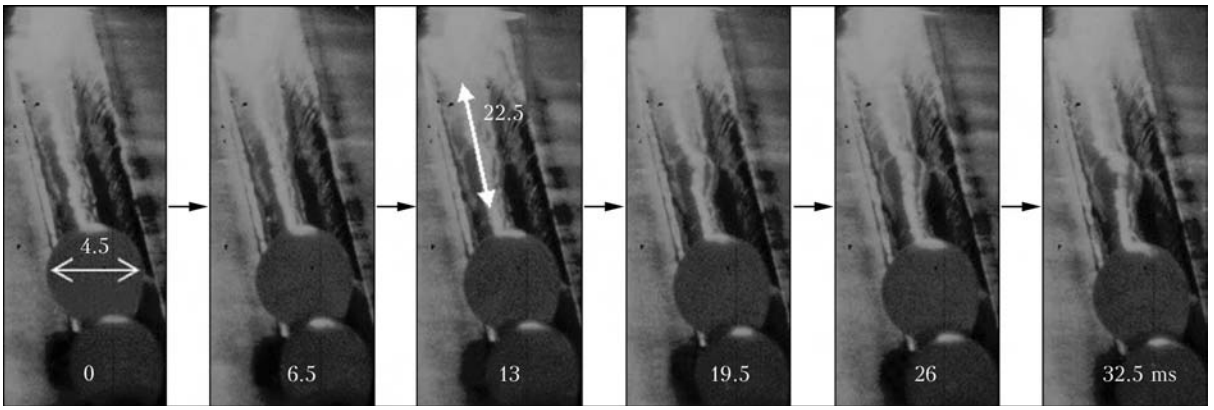

Figure 11. Dynamics of humps growth (high-speed video record of weld pool)

the scopes of investigations during welding process (Figure 11) the flow of melt was fixed in the direction to the tail of weld pool. Besides, one can observe the dynamics of development of single humps, their sizes and speed of growth (Figure 12).

It was observed that humps have definite speed of movement relative to the surface of metal plate being welded. The speed of movement of humps decreased as they grow from the order of five speeds of welding to speed of welding. The average speed of melt flow in the middle of weld pool was about 40 m/min relative to the surface of a plate. As the measurements showed, the humps grow fast at first. With increase of sizes the speed of their growth sharply decreases.

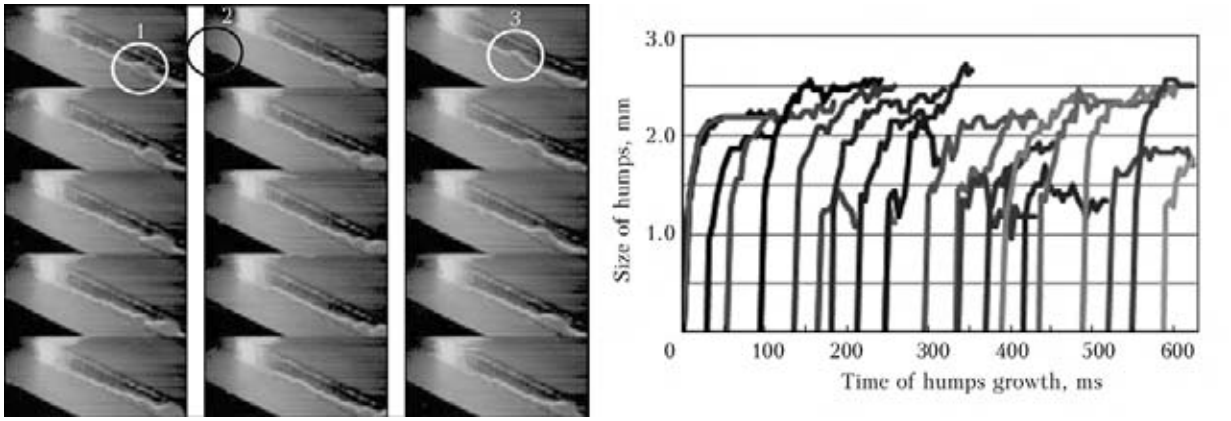

Figure 12. Dynamics of humps growth of weld pool (filming during welding process)

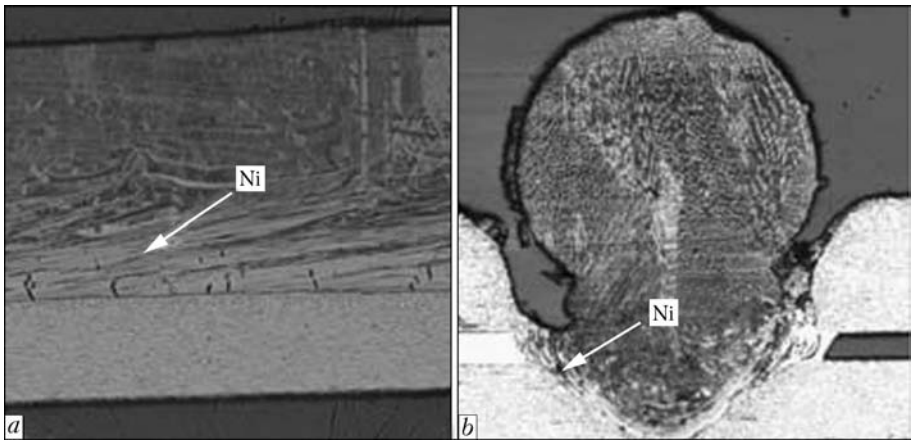

Figure 13. Distribution of nickel in weld in reflected electrons: *a* — longitudinal; *b* — transversal section of hump

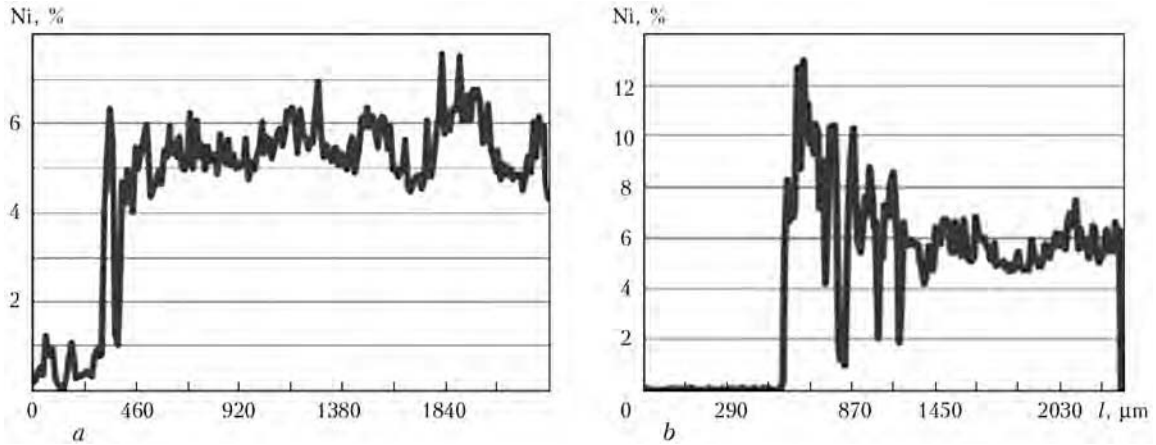

Figure 14. Distribution of nickel in a hump in horizontal (*a*) and vertical (*b*)

The measured data were numerically imposed on exponential function $\Delta\gamma = ae^{-\gamma t}$. As an average value for damping growth of humps the parameter $\gamma = 90$ s^{-1} was used. Further, on some curves under investigation the sharp deviation from constant damping growth is observed. There are single humps which stop their growth at the initial stage and are dispersed in the weld pool volume. The absorption of the small humps by large ones does also take place.

Experimental determination of melt flows in weld pool. For visualization of melt movement in weld pool the specimen was used which represented two overlap metal plates of 1 mm thickness with a thin nickel strip between them, the thickness of which was 100 μm. The similar experiments were carried out earlier on thick materials [12] where vertical flows of liquid in weld pool were observed. In our experiments the similar vertical flows were not revealed, but horizontal flows of indicator material in weld root were fixed (Figure 13).

Except of optical and metallographic investigation the microprobe power disperse analysis was carried out (Figure 14) the results of which did not reveal the gradient in concentration of nickel in the section of a hump both in longitudinal and also in transverse direction.

The given results represent the principally different dynamics of formation of weld pool surface and evidence of the fact that driving force in formation of humps in welding of thin-sheet materials is not vertical convection flows, but surface effects, first of all, the Marangoni effect.

CONCLUSIONS

1. Basing on the joint investigation of stability of hydrodynamic and thermal processes in weld pool, the model of formation of undercuts and humps on the surface of welds in NV-EBW was developed. Theoretical analysis and results of modeling showed that the cause of formation of undercuts is the surface phenomenon, and the cause of humps occurrence is the developing of instability of thermal capillary flow of melt in the weld pool.

2. The thresholds of speed of humps and undercuts formation are determined depending on beam current and working distance. It was established that with increase of beam current the instability of weld pool is increased. With decrease of working distance the intensity of beam is increased, therefore, it is necessary to decrease beam current to maintain the required penetration depth. The weld profile in this case becomes narrower and the threshold of speed of humping formation is changed negligibly.

3. The thresholds of speed of humps formation were experimentally determined for different materials. With increase of material thickness the threshold of speed of humps formation is decreased. The reason is the change in conditions of heat-mass transfer of a melt. It was established that the leading role is played by the Marangoni effect.

4. The application of surface-active substances allows suppressing of humps formation due to change of coefficient of surface tension.

5. High-speed video record allowed estimation of speed of melt flowing in weld pool, dynamics of growth and sizes of separate humps.

6. Due to application of the nickel indicator in weld pool the horizontal flows and lack of vertical ones were revealed, which was proved by results of microprobe analysis of sections in longitudinal and transverse directions.

This work was carried out within the scope of Project Di.434/88-1, LA 248/1-1 under support of Deutsche Forschungsgemeinschaft.

1. (1962) *Introduction to electron beam technology*. Ed. by R. Bakish. NY; London: John Wiley & Sons.
2. Bach, Fr.-W., Szelagowski, A., Versemann, R. et al. (2002) Non vacuum electron beam welding of light sheet metals and steel sheets. *IIW Doc. 823–02*.
3. Powers, D.E., Schumacher, B.W. (1989) Using the electron beam in air to weld conventionally produced sheet metal parts. *Welding J.*, 68(**2**), 48–53.
4. Dilthey, U., Masny, H. (2005) *Hochgeschwindigkeitsschweissen mit dem Elektronenstrahl an Atmosphaere — Fer-*

tigung von Karosseriekomponenten: DVS-Berichte, Vol. 237. Duesseldorf: DVS.
5. Bach, Fr.-W., Beniyash, A., Lau, K. et al. (2009) Non-vacuum electron beam welding of structural steels. *The Paton Welding J.*, **5**, 22–26.
6. Albright, C.E., Chiang, S. (1988) High speed laser welding discontinuities. In: *Proc. of 7th ICALEO* (Santa Clara, CA, USA, 1988), 207–213.
7. Wei, P.S. (2011) Thermal science of weld bead defects: A review. *J. Heat Transfer*, 133.
8. Turichin, G., Valdaytseva, E., Bach, Fr.-W. et al. (2010) Dynamic processes at high speed laser and electron beam treatment of materials. In: *25th Ann. of Cooperation: Transactions of St. Petersburg State Polytechnic University and Leibniz University of Hannover*, 91--101.
9. Reisgen, U., Schleser, M., Abdurakhmanov, A. et al. (2010) Messung der Strahlqualitaet einer Elektronenstrahlanlage in Umgebungsatmosphaere. *Materialwissenschaft und Werkstofftechnik*, 41(**1**), 45–52.
10. Rayleigh, J. (1945) *The theory of sound*. NY: Dover.
11. Czerner, St. (2005) *Schmelzbaddynamik beim Laserstrahl — Waermeleitungsschweissen von Eisenwerkstoffen*: Diss. Hannover.
12. Sievers, E.-R. (2006) Schmelzbadinstabilitaeten beim Elektronstrahschweissen von Grobblechen. *Schweissen und Schneiden*, 58(**6**), 288–295.

APPLICATION OF TITANIUM ALLOYS WITH SUBMICROCRYSTALLINE STRUCTURE FOR RECONDITIONING OF GTE ROTOR PARTS

A.V. OVCHINNIKOV
Zaporozhie National Technical University, Zaporozhie, Ukraine

Influence of structural condition of filler materials on the structure and properties of welds in welded joints of high-temperature titanium alloy VT8 is considered for the case of repair of aircraft engine parts. It is established that application of filler materials with submicrocrystalline structure allows ensuring an increase of the level of the joint mechanical properties.

Keywords: *argon-arc welding, titanium alloy VT8, filler materials, repair of aircraft engines, submicrocrystalline structure, weld metal, pores, mechanical properties*

Application of welding in manufacturing and repair of products from complex-alloyed titanium alloys is related to a whole number of problems. The most complex of them is welding of two-phase titanium alloys used in gas-turbine engines (GTE), as they are applied in different structural states, ensuring the required level of mechanical and service properties of material [1]. Weldability problems are related to a change of the structure of weld and HAZ metal, as well as formation of defects of weld structure (porosity, nonmetallic inclusions, chemical and structural inhomogeneity). One of the main defects is weld porosity responsible for up to 56 % of the general number of defects [2]. Weld properties and appearance of such defects as pores, nonmetallic inclusions, chemical and structural inhomogeneity in its structure directly depend on the composition and quality of filler materials. Issues related to filler material quality have gained special importance over the recent years, as complex-alloyed high-temperature titanium alloys are applied for thin-walled parts (blades, blisks, etc.) operating at the limit of material strength margin. Therefore, presence of microdefects in filler materials can lead to a complete loss of performance of the reconditioned parts. Several works describe the methods to reduce the number of defects in filler materials [3, 4]. The proposed solutions, however, pertain to surface defects and do not solve the problems of volume structural state of the fillers.

Thus, in welding of critical parts from high-temperature titanium alloys applied for GTE rotor parts, it is necessary for filler materials to provide a stable high quality of the weld. The present work deals with the influence of structural state of filler materials on the structure and properties of welds in welded joints of high-temperature titanium alloys.

Materials and investigation procedure. Welded joints of two-phase high-temperature titanium alloy VT8 were selected as an object of investigations. This alloy is used for monowheels (blisks) of high-pressure compressor (HPC) of D27 turbofan. 2 mm plates from VT8 alloy were welded by argon-arc welding by 1.8 mm nonconsumable tungsten electron in the following modes: I_w = 180 A, U_w = 10 V. VD302 power source, U6872-5306 chamber with controllable atmosphere (argon), filler materials of standard compositions (VT2 alloy wire and VT8 alloy rod) were used. 2 mm rods of the same composition, but with submicrocrystalline (SMC) structure were used as experimental filler materials. Blanks for rods with SMC structure were produced at realization of intensive plastic deformation by the method of helical extrusion with simultaneous application of normal and tangential stresses at temperatures of 400–800 °C [5, 6].

Chemical composition was studied by means of chemical analysis to GOST 19863.1-19863.13 and microanalysis in the JEOL scanning electron microscope JSM-T300. Microstructure was studied in optical microscope «Neophot-32» and transmission electron microscope JEM-100CXII at accelerating voltage of 100 kV, as well as in scanning electron microscopes JSM-T300 and REM-106I with energy dispersive